

Supervised Learning based Chest Disease Prediction with IOT from Xray Images

Spoorthi KN¹, Sahil Sarma Kuppa¹, Sree Parvathy Sajeev¹, Khushi KS¹, Kavya Ajay¹, Angulakshmi M^{2*}

¹School of Computer Science and Engineering, Vellore Institute of Technology, Vellore, India, ²School of Computer Science Engineering and Information Systems, Vellore Institute of Technology, Vellore, India. *Corresponding Author's Email: angulakshmi.m@vit.ac.in

Abstract

New WHO research indicates that there are an increasing number of chest-related illnesses. This results in the deaths of 17.9 million people annually. It gets harder to identify problems and start therapy at an early age as the population grows. However, new developments in technology, such as deep learning and machine learning methods, have sped up research in the medical profession. The creation of a machine learning and deep learning model for heart disease prediction based on pertinent features is the goal of this study. The chest's X-ray images are kept in the cloud for public access in the suggested method. The images retrieved from the cloud via the internet are analyzed for prediction using machine learning methods such as K Nearest Neighbor and Random Forest and deep learning algorithms such as Convolutional Neural Network and ResNet. Results are further stored in the cloud. Doctors, users, and patients can access the saved findings on cloud servers for diagnosis and treatment. We used a benchmark dataset from UCI Chest Disease Prediction for this research study. The proposed method classified X-ray images into normal and chest disease as cardiomegaly, aortic enlargement, and enlarged cardioment. Results are updated in the cloud for doctor diagnosis purposes. From experimental analysis, ResNet produced better results compared to other methods.

Keywords: Chest Diseases, Classification, Convolutional Neural Network, Internet of Things, K-Nearest Neighbor, Randon Forest, ResNet.

Introduction

An inexpensive and non-invasive way to examine the body's organs is via X-ray radiography (1). X-rays are frequently employed to identify a variety of diseases and anomalies. And are also useful for monitoring patients while they are receiving therapy (2). Globally, an estimated 3 billion images from X-rays are taken annually. This figure only includes the more than 150 million of the chest X-ray radiographies (CXR) that were done in the US. According to the World Health Organization (WHO), CXRs are the most widely used clinical imaging method in the world (3). Grayscale images known as CXRs are often created by beaming X-rays onto a human body that is positioned in front of a steel plate. Figure 1 shows examples of CXR images for normal, cardiomegaly, enlarged cardio mediastinum, and aortic enlargement (4). Despite being essential in the identification of thoracic diseases, radiologists' visual assessment of CXRs is still difficult and prone to inaccuracy. Prior research

has demonstrated that the longer the need for an imaging specialist to analyze CXR images, the higher the chance of error. In addition, due to concealed diseases and in the signs of skeletons and connective tissue, even seasoned radiologists were more likely to make a mistaken diagnosis (4). According to the WHO, millions of people could die from numerous chest illnesses that are potentially fatal if they are not appropriately and promptly treated (5). Certain respiratory illnesses have high death rates, such as TB, which assassinated about 1,400,000 individuals yearly; pneumonia, which destroys 900,000 youngers under those over the age of 5 and is the primary cause of death worldwide; and COVID-19, which as of November 2022 killed over 6 million people worldwide (6). In many parts of the world, there is still a severe radiology shortage, mostly due to the large number of patients who require radiological exams more quickly than new radiologists can be trained. The key factors that

This is an Open Access article distributed under the terms of the Creative Commons Attribution CC BY license (<http://creativecommons.org/licenses/by/4.0/>), which permits unrestricted reuse, distribution, and reproduction in any medium, provided the original work is properly cited.

(Received 8th August 2024; Accepted 19th January 2025; Published 27th January 2025)

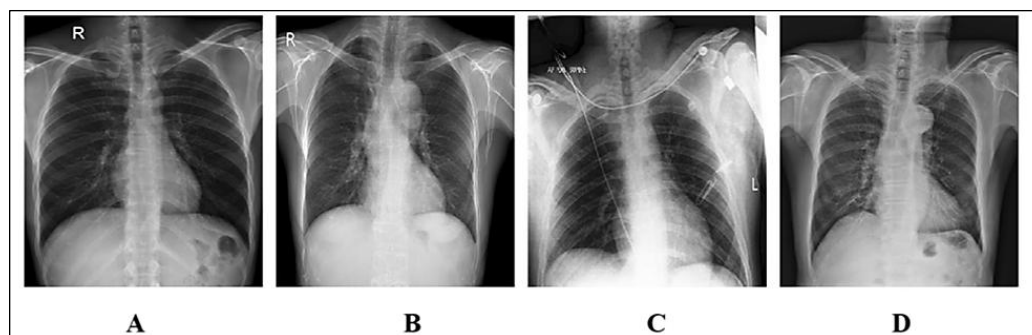


Figure 1: A) Normal B) Cardiomegaly, C) Enlarged Cardio Mediastinum, D) Aortic Enlargement (4)

emphasize the need for effective computer-assisted detection (CAD) systems for the early identification of chest diseases are the length of hospital waiting lists for diagnosis, the frequent incidence of misdiagnosis of CXR pictures, and the proliferation of life-threatening diseases (7). Because numerous illnesses are similar and a CXR is a less clear imaging modality, radiologists may not always be able to identify chest ailments on it. This results in a high probability of inaccuracy for specialists who employ visual techniques to identify illnesses. A great deal of research has been done to use image-based AI systems to address this difficulty. A thorough examination of the body of research and knowledge about the prediction of heart disease using various machine learning and deep learning approaches was part of the literature study. The latest developments and constraints of using machine learning to diagnose cardiovascular disease were examined in a number of researches. For example, various studies suggested data mining and machine learning techniques based on carotid artery images, ECG images, and heartbeat segmentation and selection processes, among other things. Applying machine learning techniques like Decision Tree, Naïve Bayes, Random Forest, Support Vector Machine, and Logistic Regression to the Heart Disease Dataset has been the focus of numerous studies, with encouraging classification accuracy rates. Furthermore, deep learning techniques—in particular, Convolutional Neural Networks, or CNN—have become increasingly popular for efficiently managing challenging assignments and unstructured data (8). By identifying hidden patterns in data, making forecasts, and enhancing performance based on past data, machine learning algorithms are essential for accurately predicting cardiac disease. These systems help us better predict and

diagnose cardiac disease, and deep learning—powered by artificial neural networks—is essential for managing intricate calculations on massive amounts of data. These algorithms are crucial for spotting important characteristics and trends in both structured and unstructured data, which promotes more effective data processing and analysis. The detection and treatment of cardiac disease may benefit greatly from the application of machine learning and deep learning techniques (9). In order to develop a universal and customized approach to healthcare, these advanced tools allow the integration of multiple data sources, including genetics, imaging data, medical records, and lifestyle factors. Machine learning's and deep learning iterative nature recognizes ongoing learning and adaptation, leading to improved diagnostic and predictive models over time. This has the potential to improve patient outcomes by increasing the precision and efficacy of heart disease care (10). A common healthcare application is remote healthcare monitoring, which aids physicians in keeping an eye on patients in remote locations who have acute or chronic illnesses, as well as hospitalized patients and elderly individuals receiving in-home care (11). Many wearable gadgets and health monitoring equipment are now easily accessible on the market as a result of the recent, swift improvements in technology. Modern technologies like the Internet of Things, machine learning, and artificial intelligence greatly simplify the work of doctors. With the assistance of modern algorithms, these technologies assist in determining the root causes of illness and determining how bad it is. The study's goal is to offer an ML methods and Deep learning models for predicting heart disease with integrating IOT devices. We thus offer a Supervised Learning based Internet of Things

Chest Disease Prediction using Xray Images. Patients can upload chest x-ray images via a network connection by using this method. After then, the photos are securely stored in cloud storage. These photos are retrieved from the cloud by an analysis of data component in order to forecast diseases. We combine machine learning and deep learning algorithms to forecast chest disorders. CNN, ResNet, Random Forest, and KNN are the models that are employed in this strategy. Results are futher stored in cloud Doctors, users, and patients can access the saved findings on cloud servers for diagnosis and treatment.

Novelty

Predicting chest disease from X-rays using the Internet of Things (IoT) is an intriguing nexus of technology and healthcare that offers a number of innovative and significant applications. Improved response time and quicker, more accurate decision-making for physicians are two benefits of the suggested IOT-based chest illness prediction. The suggested approach can be used for predictive analytics and ongoing patient monitoring. IoT technologies can track patients' health parameters continually after a diagnosis of a chest condition and notify medical professionals

of any developments. In order to make sure that patients are following treatment guidelines, this continuous data stream assists physicians in monitoring recovery or problems. Ultimately, the combination of IoT with X-ray-based chest illness prediction has the potential to transform healthcare delivery by increasing diagnostic precision, improving patient outcomes, and creating more effective healthcare systems. A smarter, quicker, and easier-to-use healthcare ecosystem is promised by the combination of real-time data, AI algorithms, and cloud-based solutions. The proposed method flow diagram is shown in Figure 2.

The following are the proposed approach's primary contributions.

- Applying the concepts of Supervised Learning Techniques (machine learning and deep learning) for improved accuracy for chest disease;
- Appropriate preprocessing is carried out to eliminate noise; and
- Increasing the model's efficacy through the combination of IOT with the prediction model.
- The proposed method increasing diagnostic precision, improving patient outcomes, and creating more effective healthcare systems.

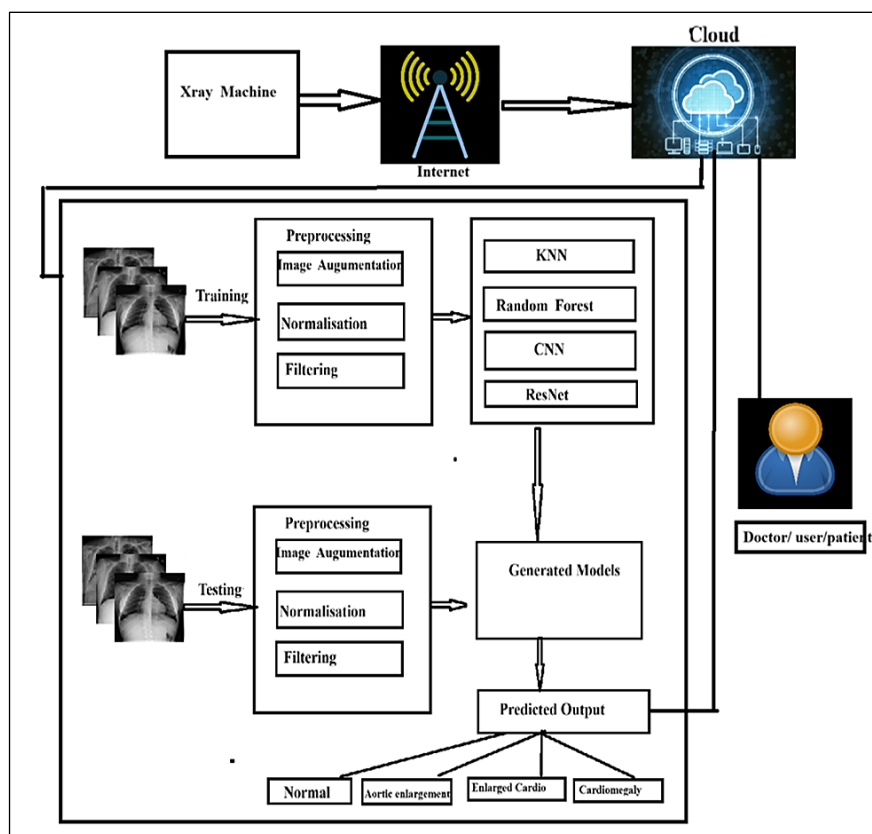


Figure 2: Proposed Method Flow Diagram

An altered DenseNet has a framework dubbed CheXNet, with 121 layers of convolution to identify 14 deviations in the chest to deal with the issue of chest overlaps disorders and to stay away from the difficulties that radiologists face (13). The model was trained and evaluated in this experiment using the ChestX-ray14 dataset. Four twenty test images were used in the set. CheXNet produced remarkable results that exceeded the level of radiologists, with a mean AUC (area under the curve) of 84.11%. and a 43.50% F1 score. Pneumothorax images from the CheXpert dataset can be diagnosed using CXR using a deep learning model called tCheXNet, which contains 122 deep layers (14). With transfer learning, CheXNet makes use of the CheXNet model (14). The model's classification of pneumothorax yielded an AUC of 70.80%. A unique DCNN model is used to identify pneumonia (15). For this experiment, a dataset of 5,856 CXR pictures was gathered via Kaggle. Using rotation, resizing, and flipping as data-augmentation strategies, the suggested model produced excellent results, with an 83.83% accuracy rate (ACC). ChestNet is a two-branch pipeline that incorporates the attention approach into its design (16). The first part of ChestNet is for the extraction of features and classification of 14 chest ailments, with a ResNet152 serving as the foundation. An attention mechanism is used in the second branch to associate class labels with the location of the disease. Chest-Net performed well, obtaining an average AUC of 78.10% when trained and evaluated using the ChestX-ray14 data. A multi-label classification technique based on a DL architecture for the detection of 14 thoracic abnormalities is present in the paper (17). The CheXpert dataset showed excellent performance from the suggested model. For the identification of five lung disorders, a mean AUC of 94.00% was attained (18). 12 chest anomalies from two publicly accessible datasets (PLCO and ChestX-Ray14) were classified using a location-aware model using CXR pictures (19). The suggested DenseNet121 model outperformed four other models—ResNet50, GoogleNet, VGG16, and AlexNet—when assessed on the identical set of data, with an average AUC of 87.40%. A method for classifying CXR images from the ChestXray14 dataset was presented using EfficientNet-V2M and transfer learning (20). Three classes were created by the model from the images: normal,

pneumonia, and pneumothorax. Having an 82.15% overall accuracy, 91.65% specificity, and 81.40% sensitivity, EfficientNet-V2M demonstrated its effectiveness. Four classes in the dataset—normal, tuberculosis, pneumothorax, and pneumonia—were used to test this model. It achieved an 82.20% mean ACC. Different DCNN models were used to categorize CXR pictures into six classes (21). Xception with the Adam optimizer was the model that performed the best. With an average AUC of 95.84%, it outperformed other DCNN models. When tested for the identification of 14 anomalies from the CheXpert dataset, this model performed well. It obtained an AUC of 94.90% overall. A DCNN model that has 201 deep layers and 20 million parameters is called DenseNet201 (22). It was a solution to deep neural networks' declining accuracy as a result of the vanishing gradient. This approach uses dense connections through dense blocks to connect all levels (each one to every other layer) in a feed-forward fashion. When tested on the ImageNet dataset, DenseNet models performed well.

Methodology

In the proposed method images of chest taken from xray machines are stored in the cloud via internet. Images from the cloud are processed by the machine learning and deep learning models and results of processing stored again in cloud for access for diagnosis by the doctor/patient. We suggested a Data Pre-processing architecture in this part. We employ machine learning and deep learning models for the chest disease diagnosis model because they excel at identifying intricate patterns in picture data and are thus well-suited for the task. But careful preprocessing is necessary to fully utilize raw photos and realize their full potential. Here is a detailed examination of some crucial techniques:

Image Augmentation

Lack of data is a common issue in deep learning. By adding new, varied variations of already-existing images to the dataset, augmentation improves model generalizability and reduces overfitting. On leaves, common techniques include rotation, flipping, scaling, cropping, color jittering, noise addition, and elastic deformations (23). Argumentation such as enhanced image, height, width shift, rotation, shearing, and horizontal flips are applied for the suggested method.

Data Normalization

Deep learning algorithms often presume standardized input values. Normalization is the process of normalizing intensity of pixels to a standard range which boosts training stability (24). The images in the dataset are standardized before being processed further.

Color Space Conversion

Red Green Blue (RGB) images can be converted to various color spaces in order to highlight unique disease-specific features. HSV emphasizes hue and saturation, making it easier to distinguish diseases based solely on color. A color perception tool called CIELAB (25) was utilized to help us discover minor symptoms.

Noise Reduction and Filtering

During capture or transmission, noise can bring confusion into Deep Learning models. Methods such as median filtering, bilateral filtering, and Gaussian filtering smoothen images while maintaining edges that are important for diagnosing diseases (26). To eliminate noise, we used Gaussian filtering in the suggested technique. In the proposed method we have applied 5 networks models and compared their results by carefully selecting and applying these data preprocessing techniques, we can prepare

our image data for optimal performance in deep learning-based chest disease from Xrays detection models. Experimentation and evaluation are key to finding the best approach for our specific needs. In this section, we proposed five transfer learning-based Deep learning models.

CNN: Pattern recognition in images is the main application for deep learning neural network topologies like convolutional networks (27). CNN is a prime example of an artificial neural network. An input, hidden, and output layer make up a typical Artificial Neural Network (ANN). These layers of a CNN are called convolutional, non-linearity, pooling, and fully connected layers. CNNs handle a lot of jobs that need image-driven pattern recognition. Advantages CNN have the ability to automatically identify and assess relevant features of images. The networks' ability to automatically adapt to the spatial arrangement of elements that the subject learns and extracts pertinent properties from the images is a crucial element of the technique. Dynamically translation invariance the capacity to detect translation invariance a method that helps verifies the existence of diseases unconnected to leaf orientation.

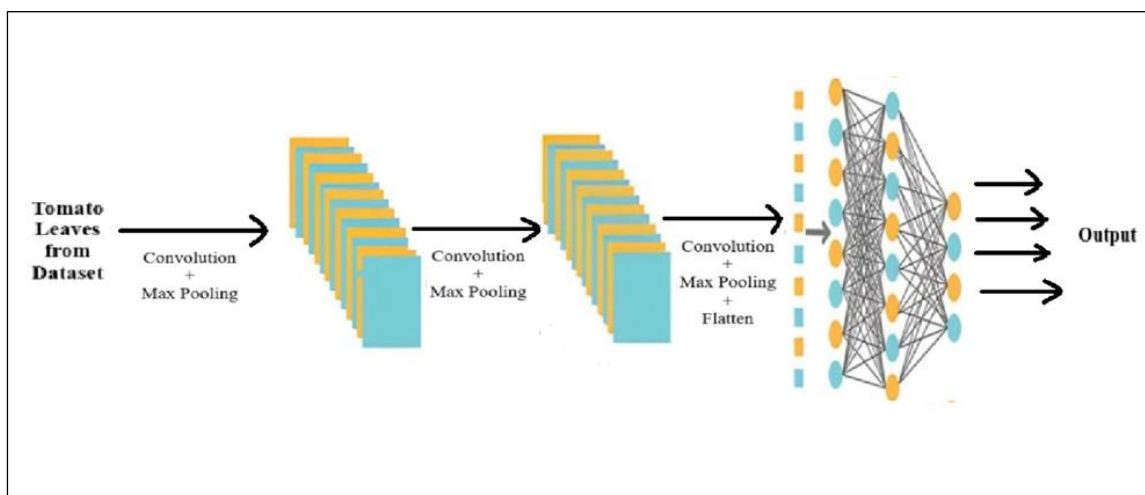


Figure 3: The Architecture of CNN (27)

CNN's input, convolution and pooling, flatten, and output layers are depicted in Figure 3 (27). First, we need to choose the architecture for our model. Three channels and a 256*256 format are used for our data input. Five is the total number of output classes that we have set, as we have five different classes in total. Our model is composed of convolutional and pooling layers initially, a 3 × 3

convolutional layer of 32 filters is present. A 2 × 2 max pooling layer follows this. By highlighting the smaller pieces, this decreases the size. Two copies of the structure are made in order to include as many 2 × 2 pooling layers as feasible. Finally, to further enhance our model, convolutional layers with 64 and 128 filters, respectively. The resulting feature map is then given a flattening layer to

make it into a flat vector. Next, a 128-neuron hidden (dense) layer is added. This is a thick, secret layer. This layer enhances the learnt qualities and helps in generalization. Finally, the output layer uses four neurons to calculate the chances between classes using the softmax activation function. We need to determine the optimal metrics and function in order to train our model. In this study, we use the Rectified Adam optimization technique. This method dynamically modifies the learning rate to enable the more efficient utilization of gradients. Furthermore, categorical cross-entropy is used as the loss of classification because it is commonly used in multiclass classification problems.

ResNet: ResNet uses skip links, informational "magic highways," in the suggested technique to compensate for vanishing gradients. Unlike ordinary roadways (convolutional layers) where information can be lost, these shortcuts ensure

that crucial visual cues concerning healthy and diseased plant tissues reach the diagnosis station (final layers). Think about the examination of leaf photos. Regular models might struggle to learn deeply nested, subtle color changes, but ResNet's shortcuts enable it to learn complex illness patterns while preserving crucial baseline knowledge. ResNet is hence a useful technique for precisely and early detection of plant diseases, potentially saving harvests and livelihoods. We have restricted the batch size to 32 and the output classes to 5 in order to accomplish this (the total number of (the total count of people who meet the requirements)). We allowed for some flexibility in figuring out the final number of input channels, which will be established by the different tests we conducted. The input image, intermediate layer, and output layers of the ResNet architecture are shown in Figure 4 (28). The same architecture was employed in the suggested method.

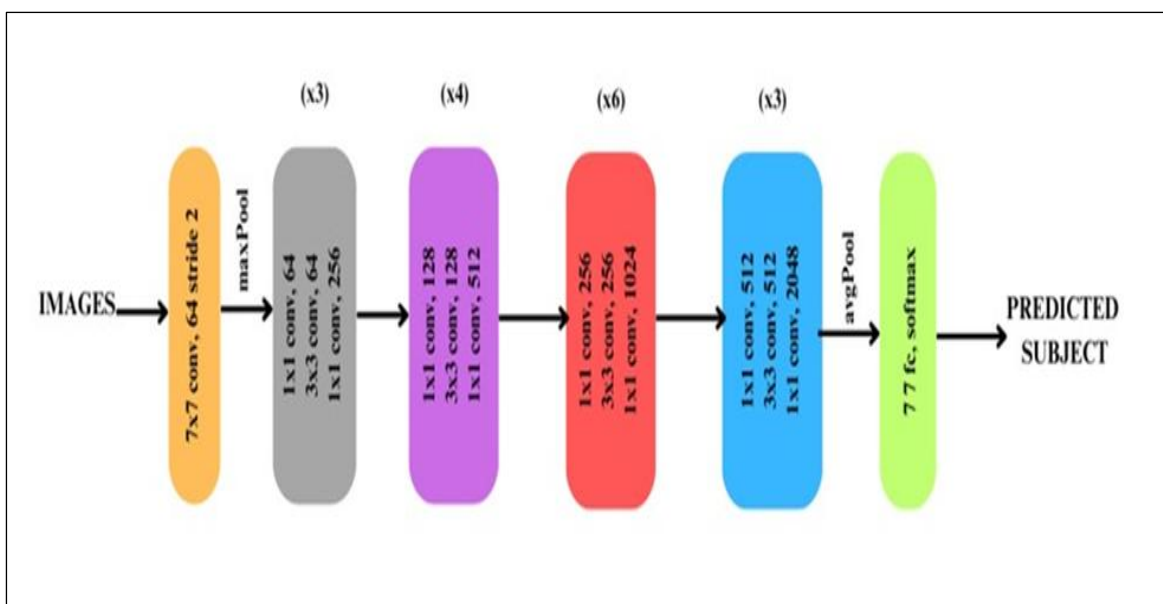


Figure 4: The Architecture of ResNet (28)

Advantages: It was one of the models that initially showed how competitive deep learning is for classifying images. Its depth allows it to capture the deeper patterns associated with illnesses of the leaves. It solves the vanishing gradient problem and allows for faster training by utilizing the ReLU activation function. It is incorporated to optimize GPU processing for quicker training.

Random Forest: A popular supervised machine learning algorithm for classification and regression issues is called random forest (29). Using various samples, it constructs decision trees and uses the majority vote for categorization and

the average vote for regression. The ability of the Random Forest Algorithm to handle data sets with continuous variables—as in regression—and categorical variables—as in classification—is one of its most crucial properties (30). It produces superior outcomes for categorization issues. Figure 5 displays the random forest architecture diagram, which includes input, output-based majority voting, and trees constructed for classes A, B, and C.

The random forest algorithm's steps are as follows:

Step 1: From the data collection containing k

records, n random records are selected using Random Forest.

Step 2: For every sample, a separate decision tree is built.

Step 3: An output will be produced by each

decision tree.

Step 4: The final product is evaluated using either regression or classification averaging, or majority voting.

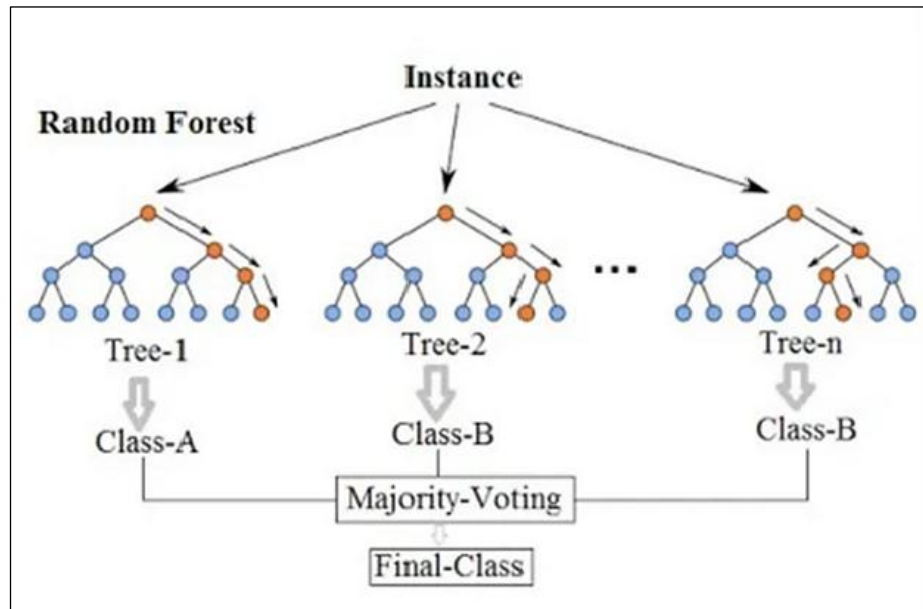


Figure 5: Random Forest (29)

K-Nearest Neighbour: An algorithm for supervised machine learning is K-Nearest Neighbor. It classifies newly discovered cases and data as most likely existing cases based on comparison with known examples. It is mostly used for classification and regression. It works well with small datasets and is memory-based. even if the number of neighbors was used to gauge its performance. Moreover, the training dataset needs to be provided appropriately because the KNN is sensitive to noisy input (31). The Euclidean distance formula is typically used to get the closest k. Eq[1] illustrates the Euclidean distance formula in the KNN method.

$$dis = \sqrt{\sum_{i=0}^n (x_{1i} - x_{2i})^2 + (y_{1i} - y_{2i})^2 + \dots} \quad [1]$$

In the given example data, y = amount of data, x = value of the x variable, y = value of the y variable, and d = Euclidean distance.

Parameter setting

The parameter setting and configuration architecture of KNN, Random Forest, CNN and ResNet are discussed below.

KNN

In order to begin the analysis, we used overall K-Nearest Neighbors (KNN) algorithm using different values for "k," which stands for the number of nearest neighbors taken into account

while making predictions. We used cross-validation to calculate scores for each "k" value and finally determined that "k = 7" produced the best mean cross-validation score. This result emphasizes how promising it is to configure KNN with "k = 7."

Random Forest

We changed the Random Forest model's tree count (n_estimators) to 200 by carrying out a thorough hyperparameter tweaking procedure.

CNN

Three layers make up the model architecture for CNN: an output layer using the sigmoid activation function, a hidden layer with 64 units using ReLU activation, and an initial layer with 128 units using the ReLU activation function. The Adam optimizer was used in conjunction with binary cross-entropy loss during model compilation, and accuracy was used as the evaluation metric.

Early halting was incorporated as a preventative step into the training procedure to lessen the possibility of overfitting. This entailed returning the model's weights to their optimal setting and tracking the validation loss for a maximum of ten epochs. Utilizing a batch size of 64, the training was carried out utilizing scaled training data for a maximum of 100 epochs.

Configuration of CNN

Convolutional Layer 1: 32 3x3 filters, stride 1, and "same" padding, ReLU Max Pooling Layer Activation: Size of pool: 2 x 2 stride 2.

Convolutional Layer 2: 64 3x3 filters with stride 1 and "same" padding, ReLU Max Pooling Layer Activation: Size of pool: 2 x 2 stride 2.

Fully Connected Layer: ReLU activation, 128 neurons

Layer of Output: One neuron with sigmoid activity for binary classification. The number of classes using softmax activation for multi-class classification

ResNet

The parameter setting of ResNet is discussed below. Prior to being augmented (original, rotated, and shifted copies of images) with a batch size of 32, the initial images used for training were downsized to 128x128x3. The ResNet model was then optimized using the random search technique, with a maximum of 30 trials

and 24 epochs. The remaining parameters were then optimized during the training of the ResNet model: "Version of ResNet," which specifies the ResNet version to be used for the model. "Batch size," which denotes the quantity of photos handled concurrently. Convergence will be sluggish if the mini-batch size is too small, and it will be slower if it is too big. The third convolutional layer's depth is denoted by "Conv3_depth." The fourth convolutional layer's depth is denoted by "Conv4_depth." One crucial hyperparameter that controls the jump's amplitude in each iteration is "learning rate." It will take a long time to converge if the learning rate is too low, and it may diverge if it is too high. The completely connected layer makes use of the "optimizer." Table 1 displays the range of hyperparameter of ResNet with version, batch size, conv3_depth, conv3_depth, and pooling, learning rate and optimizer values.

Table 1: Range of ResNet Trained Hyper parameters

Hyper parameter	Range
Version	['v1']
Batch Size	[32]
conv3_depth	[4, 8]
conv4_depth	[36]
Pooling	['avg']
Learning rate	[0.001]
Optimizer	['adam']

Results

We utilized the VinDr-CXR (4) dataset which includes the precise position of findings and the classification of various thoracic disorders. It consists of 18,000 CXR images in total. VinDr-CXR was gathered from Hanoi Medical University Hospital and H108 Hospital. A team of skilled radiologists diagnoses every dataset images. As a result, a single radiology specialist or several may diagnose two distinct diseases from the same imaging. We only keep CXR images from the VinDr-CXR dataset if a minimum of three radiologists concur that the image shows the same disease; otherwise, the image is removed.

For example, if three or more radiologists concur that the image shows single disease, the image in question is added to the proposed dataset; if not, it is going to be left out. For the purpose of classifying diseases according to afflicted organs, the images in our dataset are divided into four groups: normal, aortic enlargement, enlarged cardio mediastinum, and cardiomegaly. For the classification of specific diseases, the images are divided into 2 classes (10,606 normal cases, and 7,162 chest disease). An overview of the distribution of CXR pictures in our combined dataset is provided in Figure 6.

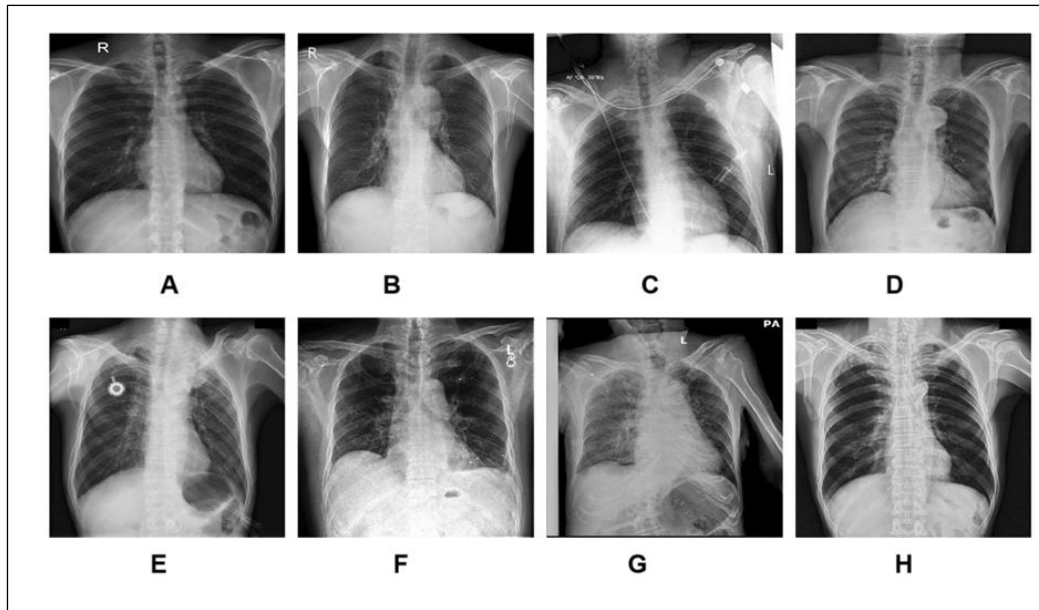


Figure 6: CXR Image Samples from our Combined Dataset: A) Normal, B) Cardiomegaly, C) Enlarged cardiomeastinum, D) Enlarged aorta, E) Aatelectasis, F) Pleural effusion, G) Pneumothorax, and H) Pulmonary fibrosis (4)

The resolution of every image was set to 256 by 256 pixels. 10% of the dataset was set aside for testing throughout the training phase, with the remaining 90% being used to train the deep learning model. Furthermore, a 10% validation split was applied to the training dataset during validation. To provide a strong model evaluation, stratified k-fold cross-validation with k=5 was used. The following indicators were used to assess the effectiveness of the suggested chest disease detection approach.

Accuracy: This measure assesses the overall accuracy of the model's predictions. It can be expressed as the proportion of correctly categorized observations to total observations. The formula to compute it is given by Eq [2].

$$Acc = \frac{TPos+TNeg}{TPos+TNeg+FPos+FNeg} \quad [2]$$

Whereas $TPos$, For instance, a t In the setting of chest disease detection, for example, a true positive occurs then the model correctly identifies an infected image as such. $TNeg$, When a healthy image is correctly classified as healthy by the model, it is an example of a true negative in the context of chest disease detection. $FPos$, A good example of a false positive in chest disease diagnosis is when the model incorrectly labels a healthy xray image as diseased (Type I error). $FNeg$, In chest disease detection, a Type II error can lead to the model incorrectly classifying a diseased as healthy. This is an example of a false

negative.

Specificity

The accuracy of the negative rate, or specificity: Specificity measures the extent to which the algorithm can detect healthy plants and distinguish between all instances of true, healthy plant cases. The equation used to compute it is provided by Eq [3].

$$Specificity = \frac{TNeg}{TNeg+FPos} \quad [3]$$

Precision

The percentage of all images that the system correctly anticipated to be disease-affected images out of all images that were favorably predicted is known as precision. The calculation formula is provided by Eq [4].

$$Precision = \frac{TPos}{TPos+FPos} \quad [4]$$

Sensitivity or Recall

The percentage of accurately predicted sick days compared to the total number of positive test case occurrences is known as sensitivity. The formula to compute it is given in Eq [5].

$$Sensitivity = \frac{TPos}{TPos+FNeg} \quad [5]$$

F1-score

The harmonic average of the two measurements, or the so-called F1-scoring system, can be used to balance recall and accuracy. The calculation formula is provided by Eq [6].

$$F1\ score = 2 * \frac{Precision*recall}{Precision+recall} \quad [6]$$

We may evaluate the efficacy and performance of

the deep learning model in reliably identifying xray images diseases and differentiating them from healthy images and anomalies by using these parameters.

Results without Image Augmentation

The proposed method used metric accuracy for

analysis of the experimental results without image argumentation techniques. Following Table 2 shows the result of the proposed method without argumentation, KNN, Random Forest, CNN and ResNet.

Table 2: The Result of the Proposed Method without Argumentation

Method	Accuracy			
	Normal	Aortic enlargement	Enlarged Mediastinum	Cardio Cardiomegaly
KNN	0.788	0.809	0.783	0.793
Random Forest	0.807	0.827	0.805	0.810
CNN	0.825	0.843	0.822	0.824
ResNet	0.839	0.858	0.839	0.838

Augmentation

In this experiment, image analysis had to be enhanced in order to determine how the amount of data impacted the generated model's accuracy. In order to conduct experiments, the performance of the model has been compared to and without augmentation. Constant hyperparameters were used during the testing process. The hidden units show the total amount of nodes required for the hidden layer. The number of input and output nodes is centered around this unit. Adam is an optimization technique derived on the lately

widely used deep learning technique known as stochastic gradient descent. The CNN algorithm, a transfer-learning method, was used in this investigation. To minimize the length of the training process, a low epoch value was chosen. 30,000 images were obtained with image augmentation, compared to around 17768 without image augmentation. Models lacking image augmentation scored lower and were consequently less adept at identifying visual patterns since there was less variance in the training data.

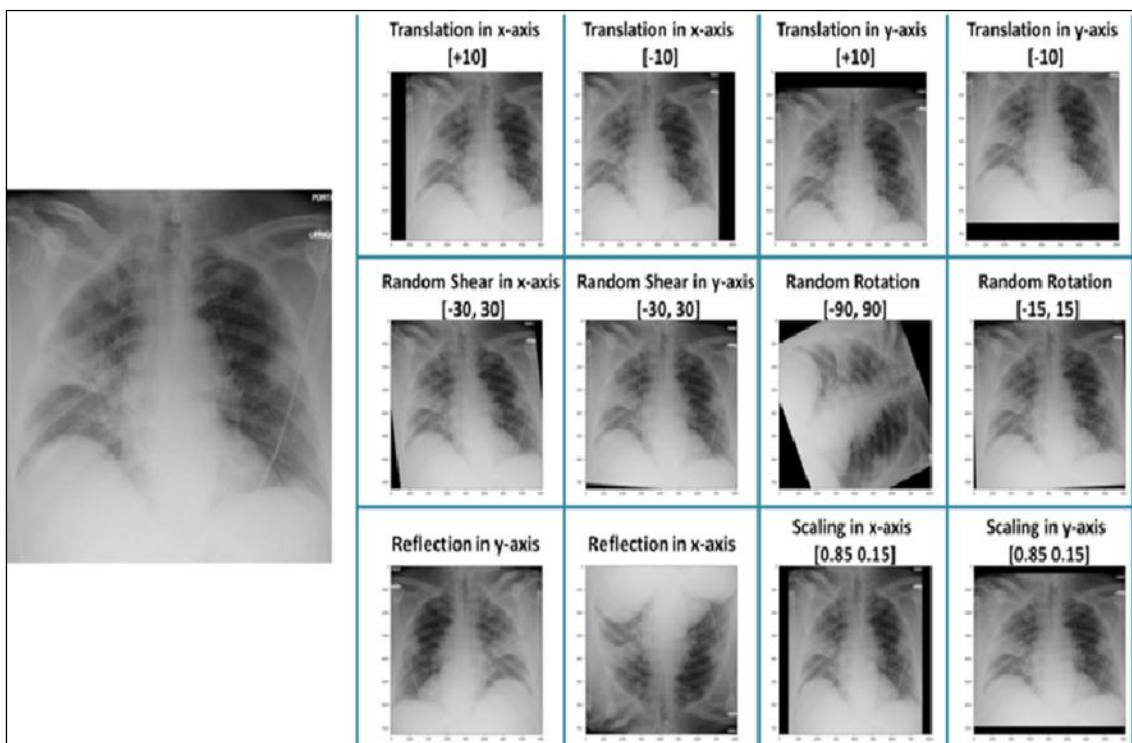


Figure 7: Augmented Results

Figure 7 displays the augmented results with scaling with the x and y axes, reflections with different axes, and rotation shear with different

angles. The key parameters of Image Argumentation for the suggested approaches are displayed in Table 3.

Table 3: Hyper parameters of Image Argumentation

Hyperparameter	
Hidden units	256
Optimizer	Adams
Epoch	100
Batch Size	64

Table 4: Comparison of Different Models for CRX Normal Images

Model	Accuracy (%)	Sensitivity (%)	Specificity (%)	Precision (%)	F1 Score (%)
KNN	89.6	86.1	93.2	92.5	89.2
Random Forest	91.8	89.6	94.1	93.7	91.6
CNN	93.5	92.2	94.8	94.5	92.8
ResNet	95.7	92.7	96.7	96.5	94.6

The categorization results for healthy images are displayed in Table 4, along with a comparison to other models. It can be concluded that, in comparison to other models, ResNet offers superior accuracy. Table 5 presents the results of

the aortic expansion of the chest and compares them to other models. It can be concluded that, in comparison to other models, ResNet offers superior accuracy.

Table 5: Comparison of Different Models for Aortic enlargement

Model	Accuracy (%)	Sensitivity (%)	Specificity (%)	Precision (%)	F1 Score (%)
KNN	91.9	94.8	92.5	92.7	93.7
Random Forest	93.5	95.4	93.7	93.9	94.7
CNN	94.7	96.5	95.1	95.2	95.9
ResNet	96.2	97.6	96.9	96.9	97.1

Table 6: Comparison of Different Models for Enlarged Cardio Mediastinum

Model	Accuracy (%)	Sensitivity (%)	Specificity (%)	Precision (%)	F1 Score (%)
KNN	89.9	85.2	93.8	93.0	88.8
Random Forest	92.4	91.2	94.6	94.4	92.6
CNN	94.1	92.8	95.4	95.2	93.9
ResNet	95.5	94.1	96.6	96.4	95.2

Table 7: Comparison of Different Models for Cardiomegaly

Model	Accuracy (%)	Sensitivity (%)	Specificity (%)	Precision (%)	F1 Score (%)
KNN	93.0	94.6	92.8	93.0	93.7
Random Forest	93.6	95.8	93.9	95.1	94.9
CNN	94.8	96.7	95.3	94.3	95.9
ResNet	96.2	97.8	96.8	96.7	96.8

Table 6 presents the classification results for enlarged cardiac mediastinum and compares them with other models. The categorization findings for the cardiomegaly are displayed in Table 7, along with the comparison with different models. The experimental research revealed that the ResNet outperformed the other techniques in

terms of results. The ResNet model's superior capacity to extract higher-level characteristics from images makes it better. Higher precision results from this. Non-linearity increased along with the number of layers with fewer kernels, a tendency that is favorable for deep learning. However, one disadvantage of ResNet is its large

number of parameters and computing demands. Table 8 shows the comparisons of the proposed

with other existing method. From the result, ResNet produced better results.

Table 8: A comparison between the Suggested Approach and Previous Research

Paper	Proposed Methods	Accuracy
(12)	Efficient Net	89.5%
(9)	CNN (8 layers: 2 fully connected, 3 max-pooling, 3 convolutional)	78%-100% (average 93.2%)
(10)	Mobile net (CNN variant)	94%
proposed	ResNet	95.7%

Discussion

KNN works well with small, straightforward datasets when interpretability is crucial, but it might not scale well with bigger data sets. The accuracy produced by the suggested method is lower than that of other methods because of the amount of the dataset. Random Forest can effectively manage bigger datasets and works well with structured/tabular data, but it is less interpretable. Computationally demanding because, particularly with big forests or datasets, prediction and training processes can be sluggish. Memory Usage: To store every tree in the ensemble, additional memory is needed. While RF outperformed KNN in terms of results, CNN and Resnet outperformed it in terms of classification accuracy. When it comes to tasks that call for hierarchical or spatial feature learning, they frequently perform worse than CNNs. When dealing with complicated, high-dimensional, unstructured data—particularly images or sequences—CNNs typically perform better than Random Forests. Despite their need for massive datasets and processing capacity, CNNs are the preferred models for image-related tasks since they automatically extract features and patterns from data. However, CNNs usually have trouble going deeper in the suggested approach since extra layers can produce problems like vanishing or expanding gradients. This hinders the effective learning of very deep networks. Consequently, the results were less accurate than those of ResNet. ResNet is a sophisticated CNN version that enables the efficient training of very deep networks, producing state-of-the-art outcomes in vision challenges. ResNet is a substantial advancement in deep model training, even though conventional CNNs are fundamental and useful for many tasks. Key issues like disappearing gradients are addressed by its architecture, which enables more precise and reliable models,

especially for intricate jobs that call for deeper networks. Because of this, ResNet frequently performs better than conventional CNNs in terms of accuracy and training stability.

Limitations

The use of IoT (Internet of Things) for X-ray image-based chest illness prediction can present a number of difficulties because of biases in the dataset and practical implementation problems. We'll go over some of the main issues in these areas below:

Class Imbalance and Dataset Bias: X-ray datasets frequently experience class imbalance. Because of this imbalance, the model may be biased toward predicting the majority class (healthy individuals), which might result in poor model performance for rare diseases.

Age and Gender Bias: Images from particular age groups or genders may be overrepresented in datasets. The model's ability to generalize to underrepresented groups may be impacted by the bias this introduces. **Geographic and Demographic Bias:** Images of medical conditions might differ significantly between institutions or various locations. If the majority of the photos in a dataset are from a single region, the model may not fit patients from other regions effectively. Bias in Quality and Resolution Models that have been trained on high-quality photos may not function effectively when exposed to low-quality photographs from less sophisticated real-world equipment.

Incomplete or Missing Data: Incomplete or missing data is a common feature of real-world datasets, and improper handling of this data can result in biases.

Challenges in Real-World Implementation

Data Collection and Labeling: Obtaining a large and diverse dataset of X-ray images with proper labeling is a significant challenge. Data labeling typically requires expert radiologists, which can

be time-consuming and expensive. Additionally, mislabeling can occur, which negatively impacts the model's accuracy. As sharing and accessing medical data across different hospitals, research institutions, or IoT devices requires addressing legal, privacy, and security concerns. This can slow down the development of IoT-based systems for chest disease prediction. A model that works well on a controlled dataset may struggle when deployed in real-world settings due to variability in X-ray images. Transfer learning techniques can help but may not always fully address these issues. Model Interpretability is another challenge to be faced. Many deep learning models used in medical applications are frequently regarded as "black boxes," which makes it challenging for medical professionals to understand the outcomes. To enable real-time predictions, IoT systems frequently include sensors, cloud services, and edge devices. However, a major engineering problem is making sure the system functions effectively, scales adequately, and delivers dependable results in real-time. Although there is a lot of promise in integrating IoT and X-ray pictures to forecast chest ailments, there are a number of issues that need to be resolved to make sure the technology is dependable, moral, and scalable in practical settings. To make these systems a useful tool in clinical settings, several significant challenges must be addressed, including dataset bias, the complexity of real-world situations, regulatory barriers, and problems with model dependability and interpretability.

Conclusion

In order to forecast various chest diseases from xrays, we used both deep learning models and Machine learning in this work. Among the deep learning models that are employed are CNN, and ResNet. Machine learning model used are KNN and random forest. Chest disease prediction is now possible with speed and accuracy thanks to the combination of deep learning and Machine learning. With an accuracy of 95.7% for normal chest images, 96.2% for Aortic enlargement, 95.3 percent for Enlarged Cardio Mediastinum, 96.2% for Cardiomegaly, ResNet outperformed all the other mode.

Abbreviations

IoT: Internet of Things, CNN: Convolutional Neural

Networks, ResNet: Residual Network, KNN: K Nearest Neighbor, DL: Deep Learning, CRX: Chest Xray.

Acknowledgement

Nil.

Author contribution

All Authors contributed the entire manuscript in writing, reviewing, implementing, Conceptualization and Analysis.

Conflict of Interest

The authors declare no conflict of interest.

Ethics Approval

The research does not involve human participants.

Funding

No funds received.

References

1. Bharati S, Podder P, Mondal R, Mahmood A, Raihan-Al-Masud M. Comparative performance analysis of different classification algorithm for the purpose of prediction of lung cancer. *Advances in intelligent systems and computing*, Springer. 2020; 941: 447-4
2. Coudray N, Ocampo PS, Sakellaropoulos T, Narula N, Snuderl M, Fenyö D, Moreira AL, Razavian N, Tsirigos A. Classification and mutation prediction from non-small cell lung cancer histopathology images using deep learning. *Nature medicine*. 2018;24(10):1559-67.
3. Liu B, Liu Y, Zhang W, Tian Y, Kong W. Spectral swin transformer network for hyperspectral image classification. *Remote Sensing*. 2023 ;15(15):3721.
4. Ait Nasser A, Akhloufi MA. A review of recent advances in deep learning models for chest disease detection using radiography. *Diagnostics*. 2023;13(1):159.
5. Ghali R, Akhloufi MA, Mseddi WS. Deep learning and transformer approaches for UAV-based wildfire detection and segmentation. *Sensors*. 2022;22(5):1977-1921
6. Cohen M, Levine SM, Zar HJ. World Lung Day: impact of "the big 5 lung diseases" in the context of COVID-19. *Am J Physiol Lung Cell Mol Physiol*. 2022;323(3): L338-L340.
7. Tsuneki M. Deep learning models in medical image analysis. *J Oral Biosci*. 2022;64(3):312–20.
8. Demner-Fushman D, Kohli MD, Rosenman MB, Shooshan SE, Rodriguez L, Antani S, Thoma GR, McDonald CJ. Preparing a collection of radiology examinations for distribution and retrieval. *J Am Med Inform Assoc*. 2016;23(2):304–1.
9. Li F, Zhou L, Wang Y, Chen C, Yang S, Shan F, Liu L. Modeling long-range dependencies for weakly supervised disease classification and localization on chest X-ray. *Quantitative Imaging in Medicine and Surgery*. 2022 ;12(6):3364.
10. Nguyen HQ, Lam K, Le LT, Pham HH, Tran DQ, Nguyen DB, Le DD, Pham CM, Tong HT, Dinh DH, Do

- CD. VinDr-CXR: An open dataset of chest X-rays with radiologist's annotations. *Scientific Data*. 2022;9(1):429.
11. P Ko HY, Tripathi NK, Mozumder C, Muengtawepongsa S, Pal I. Real-Time Remote Patient Monitoring and Alarming System for Noncommunicable Lifestyle Diseases. *International Journal of Telemedicine and Applications*. 2023;2023(1):9965226.
 12. Zhu CS, Pinsky PF, Kramer BS, Prorok PC, Purdue MP, Berg CD, Gohagan JK. The prostate, lung, colorectal, and ovarian cancer screening trial and its associated research resource. *JNCI*. 2013;105(22):1684–93.
 13. Johnson AE, Pollard TJ, Berkowitz SJ, Greenbaum NR, Lungren MP, Deng C-Y, Mark RG, Horng S. Mimic-cxr, a de-identified publicly available database of chest radiographs with free-text reports. *Sci Data*. 2019;6(1):1–8.
 14. Alfarghaly O, Khaled R, Elkorany A, Helal M, Fahmy A. Automated radiology report generation using conditioned transformers. *Informatics in Medicine Unlocked*. 2021;24:100557.
 15. Sze-To A, Riasatian A, Tizhoosh HR. Searching for pneumothorax in x-ray images using autoencoded deep features. *Scientific reports*. 2021 ;11(1):9817.
 16. Mujahid M, Rustam F, Álvarez R, Luis Vidal Mazón J, Díez ID, Ashraf I. Pneumonia classification from X-ray images with inception-V3 and convolutional neural network. *Diagnostics*. 2022 May 21;12(5):1280.
 17. Wang H, Xia Y. Chestnet: A deep neural network for classification of thoracic diseases on chest radiography. 2018; 2(1): 1807. 03058.
 18. Pham HH, Le TT, Tran DQ, Ngo DT, Nguyen HQ. Interpreting chest X-rays via cnns that exploit hierarchical disease dependencies and uncertainty labels. *Neurocomputing*. 2021; 437:186–9.
 19. Çallı E, Sogancioglu E, van Ginneken B, van Leeuwen KG, Murphy K. Deep learning for chest X-ray analysis: A survey. *Medical Image Analysis*. 2021;72:102125.
 20. Kim S, Rim B, Choi S, Lee A, Min S, Hong M. Deep learning in multi-class lung diseases' classification on chest X-ray images. *Diagnostics*. 2022;12(4):915.
 21. Meem AT, Khan MM, Masud M, Aljahdali S. Prediction of Covid-19 Based on Chest X-Ray Images Using Deep Learning with CNN. *Computer Systems Science & Engineering*. 2022 Jun 1;41(3): 1-20. <https://doi.org/10.32604/csse.2022.021563>
 22. Zhao X, Wang L, Zhang Y, Han X, Deveci M, Parmar M. A review of convolutional neural networks in computer vision. *Artificial Intelligence Review*. 2024 Mar 23;57(4):99.
 23. Fei-Fei L, Deng J, Li K. ImageNet: Constructing a large-scale image database. *Journal of vision*. 2009;9(8):1037-.
 24. Nigam S, Jain R. Plant disease identification using Deep Learning: A review. *Indian Journal of Agricultural Sciences*. 2020; 90 (2): 249–57.
 25. Litjens G, Kooi T, Bejnordi BE, Setio AA, Ciompi F, Ghafoorian M, Van Der Laak JA, Van Ginneken B, Sánchez CI. A survey on deep learning in medical image analysis. *Medical image analysis*. 2017; 42:60-88.
 26. Mukhopadhyay S, Paul M, Pal R, De D. Tea leaf disease detection using multi-objective image segmentation. *Multimedia Tools and Applications*. 2021; 80:753-71.
 27. Jung M, Song JS, Shin AY, Choi B, Go S, Kwon SY, Park J, Park SG, Kim YM. Construction of deep learning-based disease detection model in plants. *Scientific Reports*. 2023;13(1):7331.
 28. Yamashita R, Nishio M, Do RK, Togashi K. Convolutional neural networks: an overview and application in radiology. *Insights into imaging*. 2018; 9:611-29.
 29. Padshetty S, Ambika. Leaky ReLU-ResNet for Plant Leaf Disease Detection: A Deep Learning Approach. *Engineering Proceedings*. 2023;59(1):39.
 30. Sumwiza K, Twizere C, Rushingabigwi G, Bakunzibake P, Bamurigire P. Enhanced cardiovascular disease prediction model using random forest algorithm. *Informatics in Medicine Unlocked*. 2023; 41:101316.
 31. Thanh Noi P, Kappas M. Comparison of random forest, k-nearest neighbor, and support vector machine classifiers for land cover classification using Sentinel-2 imagery. *Sensors*. 2017;18(1):18